Volumetric Behavior of Athermal Dendritic Polymers: Monte Carlo Simulation

L. Lue

Physical and Chemical Properties Division, M/S 838, National Institute of Standards and Technology, 325 Broadway, Boulder, Colorado 80303-3328

Received August 9, 1999; Revised Manuscript Received October 25, 1999

ABSTRACT: We present results of Monte Carlo simulations for dilute to concentrated solutions of athermal, homogeneous dendritic polymers. The dendritic polymers are composed of tangent hard-spheres and vary from generation 0 to generation 5. These simulations investigate the effect of hyperbranching on the structure and thermodynamics of polymer solutions. At low concentrations, dendritic polymers systems have a lower pressure than linear polymers of the same molecular weight, owing to the more compact architecture of the dendrimer. In the concentrated polymer regime, solutions containing low-generation dendrimers behave similarly to linear polymers, while those containing high-generation dendrimers have a pressure that increases more rapidly with concentration.

1. Introduction

Dendrimers are highly branched polymers with a very symmetrical three-dimensional structure. They possess a central molecular group that has many "arms." Each of these arms branches into two or more arms, which in turn can branch further, etc.; the number of times that each arm branches is called the "generation number" of the dendrimer. Dendrimers are highly monodisperse owing to the careful stepwise method used to synthesize them. Several reviews on dendrimer synthetic techniques are available in the literature.[1−3]

Because of the ability to control their chemical structure and architecture, these regularly branched macromolecules can find a variety of applications, for example as adhesive and rheology modifiers,[4] advanced catalysts,[5] agents in molecular encapsulation,[6,7] building blocks for supramolecular chemistry[8] or chemical sensors.[9]

Although the synthesis of dendrimers has progressed very rapidly, studies on their physical properties are still few in number. In particular, it would be interesting to make a direct comparison between linear and dendritic polymers, because the molecular architecture and the numerous terminal surface groups of dendrimers should lead to new properties and interesting applications.

Some experimental work has been done on the structure of isolated dendrimers,[10−13] dendrimer rheology in the molten state,[14,15] thermal properties,[16] intrinsic viscosity,[17] intermolecular interactions of dendrimers in solution,[18] and thermodynamics of solutions of dendrimers.[19] However, experimental studies are hindered by the sparse availability of dendrimers and the time-consuming synthesis required to make them.

Most previous theoretical work has focused on determining the structure of isolated macromolecules. These include mean-field[20,21] and renormalized field theory models[22] as well as computer simulation studies.[23−27] Many theories exist for the thermodynamics of branched polymer systems.[28−32] However, they predict little to no influence of molecular architecture on the thermodynamics of the system, even in the case of the hyperbranched dendritic polymer. Simulations for branched molecules, in general, are rather scarce.[30,33] To our knowledge, there are no simulation studies for concentrated dendrimer solutions.

In this paper, we report Monte Carlo simulations for athermal solutions of dendritic polymers (generation 0−5) and investigate the structural and thermodynamic properties of these systems from the dilute to concentrated (up to 0.3 polymer volume fraction) regimes. Owing to the compact architecture of the dendrimer, we find that, at low concentrations, the dendritic polymer solutions have a lower pressure than the corresponding linear polymer solutions. At moderate to high concentrations, the pressure of the low-generation dendrimer solutions is almost identical to that of linear polymer solutions. For higher-generation dendrimers, the pressure increases more rapidly with concentration than that of the corresponding linear polymers.

The remainder of this paper is organized as follows. In section 2, we present the details of the simulations for the dendritic polymers. In section 3, we discuss the basic properties of linear polymer solutions. In section 4, we present and discuss the results of our Monte Carlo simulations for the dendrimers. Finally, in section 5, we summarize the major results of this paper.

2. Simulation Details

In this work, we model the polymers as a collection of tangent hard-spheres of diameter σ. These hard spheres are not allowed to interpenetrate, and, therefore, the distance between the centers of two hard spheres cannot be closer than σ. The dendritic polymers that we study have a central core that branches off into three arms. Each arm branches into two additional branches. These dendrimers are described by two numbers: the separator length and the generation number. The generation number represents the number of times each of the arms branches. The separator length is the distance between branch points. A schematic drawing of generation-0, 1, 2, and 3 dendritic polymers is given in Figure 1. This model of the dendrimer is slightly different from the one used in our previous work (see ref 27). In that study, the bond angles at the branch sites were held fixed, while, in the present work, the molecules are fully flexible.

10.1021/ma991340b
Published on Web 03/01/2000

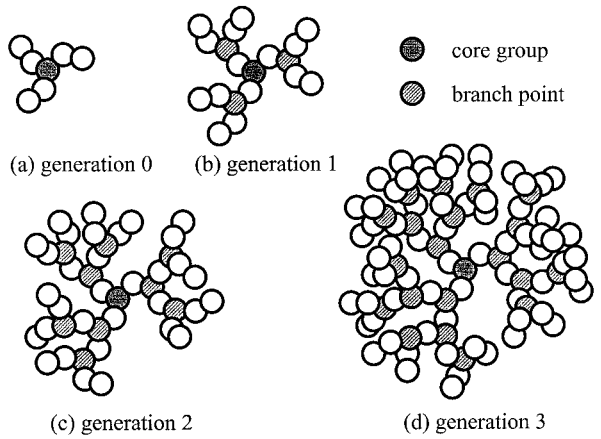

Figure 1. Schematic drawing of model dendritic polymers: (a) generation 0, (b) generation 1, (c) generation 2, and (d) generation 3. The shaded spheres represent the core molecule, and the cross-hatched spheres represent branch sites.

This model for the intermolecular interactions describes homogeneous polymers in a good solvent. We study generation-0 to generation-5 dendritic polymers with a separator length of one sphere. Two factors prevent the study of higher-generation dendrimers. The first is that the internal sections of the dendrimers become harder to equilibrate, owing to the congestion of the surfaces of the dendrimers as a result of the hyperbranching. The other factor is that the number of spheres increases dramatically with generation number. This results in a system size that quickly becomes unmanageable with current computer resources.

Simulations were performed for infinitely dilute dendrimers and linear chains of the same molecular weight. Single-polymer configurations were generated using pivot moves[27,34] and extended continuum configuration bias (ECCB) moves.[35] For each of these calculations, 10 distinct runs were performed. Each run was begun with the molecule in a fully extended conformation. Then, the molecule was equilibrated for a period consisting of 5×10^5 attempted moves (N.B., each attempted move consists of an attempted pivot and ECCB move.). The single-molecule properties were then collected from a production run of 7.5×10^6 attempted moves. During each run, configurations were saved every 10^4 attempted moves; a total of 750 single-molecule configurations were saved from each run. From these simulations, we were able to compute the conformational properties of the isolated polymers, such as the mean-square radius of gyration $\langle R_g^2 \rangle$ and the density profile.

In addition, by pairing the various single-chain configurations with one another, the potential of mean force $w(r)$ and the second-virial coefficient B_2 were computed using the method described in ref 34. In order to compute $w(r)$, two single-molecule configurations, which were generated previously, are placed such that their center of masses are a separated by a distance r. In addition, each of these single-chain configurations is randomly rotated about its respective center of mass. Then, it is checked whether this pair of molecules overlaps. This process is repeated until all of the 750 conformations, saved from the single-chain run, have been paired with each other. The potential of mean force is then given by[27,34]

$$w(r) = -k_B T \ln \frac{N_{miss}}{N_{total}} \quad (1)$$

Table 1. Mean-Square Radius of Gyration of Isolated Dendritic and Linear Polymers

generation	N	dendrimer	linear
0	7	1.3443 ± 0.0001	1.7405 ± 0.0005
1	19	3.7378 ± 0.0008	6.792 ± 0.004
2	43	7.461 ± 0.007	19.61 ± 0.02
3	91	12.85 ± 0.01	50.31 ± 0.04
4	187	20.58 ± 0.07	122.0 ± 0.1
5	379	31.9 ± 0.2	287.50 ± 0.04

Table 2. Second Virial Coefficients of Dendritic and Linear Polymers

generation	N	dendrimer	linear
0	7	35.8 ± 0.5	51 ± 1
1	19	154.5 ± 0.9	220 ± 2
2	43	482 ± 5	780 ± 28
3	91	1243 ± 5	2635 ± 64
4	187	2863 ± 44	9127 ± 85
5	379	5669 ± 123	30268 ± 513

where k_B is the Boltzmann constant, T is the absolute temperature of the system, N_{miss} is the total number of pairs that do not overlap, and N_{total} is the total number of pairs used in the calculations. The second virial coefficient can be calculated from $w(r)$ through the relation[27,34]

$$B_2 = -\frac{2\pi}{3} \int_0^\infty dr\, r^2 \{\exp[-w(r)/(k_B T)] - 1\} \quad (2)$$

The uncertainty of the simulation data was estimated from the standard deviations of the results from independent runs. The results for $\langle R_g^2 \rangle$ (in units of σ^2) are summarized in Table 1, and the results for the second-virial coefficient (in the units of σ^3) are summarized in Table 2. Note that our results for the linear chains compare well with the results of ref 34.

The simulations for concentrated dendritic polymer solutions were performed in the ensemble of constant number, volume, and temperature (NVT). In these simulations, the system is equilibrated using several types of moves. The first move is a simple random translation of the entire molecule.[36] In addition, to equilibrate the molecule itself, we employ pivot moves,[27,34] and ECCB moves.[35] To increase the efficiency of the simulations, link cells are used.[36]

In these NVT simulations, the pressure of the system is obtained by a method proposed by Eppenga and Frenkel[37] for hard-core systems. In this method, a histogram is computed for the quantity $P_1(\Delta\rho)$, which is the probability density that a given molecule will overlap with one of its neighbors, given that the density of molecules in the system is increased by $\Delta\rho$. For small values of $\Delta\rho$, P_1 has the following form[37]

$$P_1(\Delta\rho) = \alpha \exp(-\alpha\Delta\rho) \quad (3)$$

where ρ is the number density of molecules in the system and α is a constant directly related to the pressure of the system by[37]

$$\frac{p}{\rho k_B T} = 1 + \frac{\rho\alpha}{2} \quad (4)$$

where p is the pressure of the system. The function P_1 can be found by determining, for each molecule in the system, the volume change required to cause its first overlap with another molecule.

Table 3. Mean-Square Radius of Gyration

	generation					
y	0, $N = 7$	1, $N = 19$	2, $N = 43$	3, $N = 91$	4, $N = 187$	5, $N = 379$
0.00	1.3443 ± 0.0001	3.7378 ± 0.0008	7.461 ± 0.007	12.85 ± 0.01	20.58 ± 0.07	31.9 ± 0.2
0.05	1.3418 ± 0.0003	3.742 ± 0.002	7.416 ± 0.009	12.76 ± 0.03	20.46 ± 0.07	31.7 ± 0.1
0.10	1.3307 ± 0.0002	3.661 ± 0.003	7.19 ± 0.01	12.22 ± 0.04	19.46 ± 0.06	30.5 ± 0.1
0.15	1.3177 ± 0.0002	3.568 ± 0.003	6.89 ± 0.03	11.50 ± 0.07	18.0 ± 0.1	27.9 ± 0.1
0.20	1.3017 ± 0.0003	3.465 ± 0.005	6.58 ± 0.04	10.8 ± 0.1	16.6 ± 0.2	25.23 ± 0.07
0.25	1.2813 ± 0.0006	3.356 ± 0.007	6.30 ± 0.06	10.2 ± 0.1	15.5 ± 0.2	23.75 ± 0.08
0.30	1.254 ± 0.001	3.24 ± 0.01	6.05 ± 0.09	9.7 ± 0.1	14.8 ± 0.1	22.6 ± 0.08

Table 4. Pressure of Dendritic Polymer Solutions

	generation					
y	0, $N = 7$	1, $N = 19$	2, $N = 43$	3, $N = 91$	4, $N = 187$	5, $N = 379$
0.00	0	0	0	0	0	0
0.05	0.0241 ± 0.0003	0.0113 ± 0.0002	0.0069 ± 0.0002	0.0042 ± 0.0002	0.0025 ± 0.0001	0.00141 ± 0.00006
0.10	0.079 ± 0.001	0.049 ± 0.002	0.035 ± 0.002	0.029 ± 0.001	0.0228 ± 0.0008	0.0176 ± 0.0007
0.15	0.186 ± 0.004	0.131 ± 0.002	0.112 ± 0.006	0.108 ± 0.006	0.092 ± 0.005	0.084 ± 0.003
0.20	0.372 ± 0.006	0.296 ± 0.006	0.280 ± 0.006	0.267 ± 0.014	0.26 ± 0.01	0.244 ± 0.008
0.25	0.69 ± 0.01	0.596 ± 0.013	0.56 ± 0.02	0.55 ± 0.04	0.56 ± 0.02	0.56 ± 0.02
0.30	1.24 ± 0.03	1.09 ± 0.03	1.05 ± 0.06	1.06 ± 0.06	1.07 ± 0.04	1.15 ± 0.05

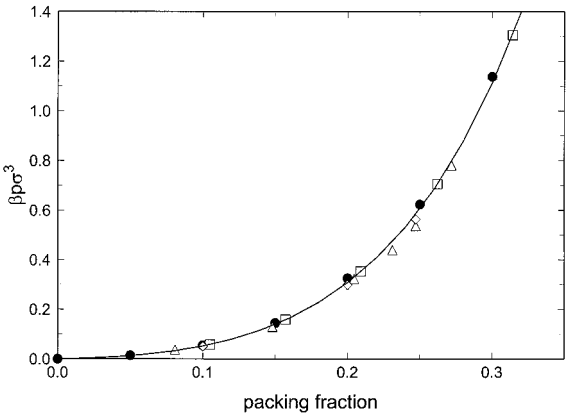

Figure 2. Equation of state for tangent hard-sphere chains with $N = 16$: (i) present work (filled circles), (ii) Dickman and Hall[38] (open triangles), (iii) Gao and Weiner[39] (open squares), (iv) Denlinger and Hall[40] (open diamonds), and (v) TPT-D1 equation of state for $N = 16$ (solid line).

This method for determining the pressure of a system was originally developed for nonspherical hard-core molecules. It is also applicable to flexible molecules, although, to our knowledge, it has been applied only to rigid molecules. Therefore, to verify the validity of this method for obtaining the pressure of flexible molecules, we compute the equation of state of linear tangent hard-sphere chains composed of 16 spheres using NVT Monte Carlo simulations with 100 chains. The results are presented in Figure 2 and compared to the results obtained by other researchers. Our Monte Carlo (MC) results (filled circles) compare well to those of other authors[38−40] (open symbols), confirming the applicability of this method to flexible molecules.

For the dendrimers of generation 0 and 1, NVT Monte Carlo simulations were performed with 100 molecules. For generations 2−5, the simulations were performed with 27 molecules. Standard periodic boundary conditions were used in all the many-polymer simulations. Each of the simulations began with an equilibration period consisting of 5×10^7 attempted moves. Then simulations were divided into separate runs, each consisting of 10^7 attempted moves (where an attempted move is one trial each of the random translation, pivot, and ECCB moves), over which system property data (such as the pressure) were collected. At least 20 runs, and up to 100, were performed for each system. The uncertainty of the simulation data was estimated from the standard deviations of the results of separate runs from the mean. The results for the mean-square radius of gyration (in units of σ^2) are presented in Table 3, and the results for the pressure (in units of $k_B T/\sigma^3$) computed from our simulations are presented in Table 4.

3. General Considerations

In good solvent conditions, solutions of linear polymers exhibit three major regimes:[41,42] (i) the dilute regime, (ii) the semidilute regime, and (iii) the concentrated regime.

In the dilute regime, the polymer concentration is low enough that the polymers rarely interact with each other. In this regime, the polymers behave as individual molecules, and the truncated virial expansion accurately describes the properties of the system. The relevant length scale that describes the physics of this regime is the size of the individual polymers.

In the semidilute regime, the polymer volume fraction is still small; however, because of the large size of the individual polymer coils, the polymer chains now interact significantly with each other, and the truncated virial expansion no longer accurately describes the system. In this regime, the polymers no longer exist as individual molecules, but instead form an interpenetrating network. Here, the relevant length scale is the mesh size of the network. In this regime, the properties of the solution exhibit scaling behavior.[41,42]

In the concentrated regime, the polymers now occupy a significant volume fraction of the system. In this regime, unlike the previous two regimes, the details of the monomer−monomer interaction play a significant role. There has been a lot of simulation[38−40] and modeling[32,43−48] work for linear tangent hard-sphere systems in the concentrated regime. In this regime, the TPT-D1 equation of state[47] has been found to work well for these systems

$$Z = NZ_{HS} - \frac{N}{2}\left(1 + y\frac{\partial \ln g_{HS}(\sigma)}{\partial y}\right) - \left(\frac{N}{2} - 1\right)\left(1 + y\frac{\partial \ln g_{HD}(\sigma)}{\partial y}\right) \quad (5)$$

where ρ is the number density of chains, N is the

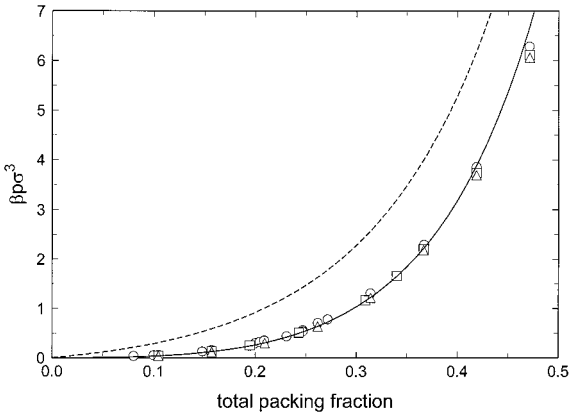

Figure 3. Equation of state for tangent hard-sphere chains: (i) $N = 16$[38−40] (circles), (ii) $N = 51$[39] (squares), (iii) $N = 201$[39] (triangles), (iv) hard spheres, as predicted by the Carnahan−Starling equation of state (dashed line), and (v) infinitely long chains, as predicted by the TPT-D1 equation of state (solid line).

number of spheres per chain, $y = \pi\sigma^3 N\rho/6$ is the fraction of space occupied by the spheres, σ is the diameter of the spheres, $g_{HS}(\sigma)$ is the contact value of the pair-correlation function of a hard-sphere fluid, $g_{HD}(\sigma)$ is the contact value of the site−site pair-correlation function of a tangent hard-dumbbell fluid, Z is the compressibility factor of the system, and Z_{HS} is the compressibility factor of a hard-sphere fluid. The equation of state of hard spheres is well represented by the Carnahan−Starling equation:[49]

$$Z_{HS} = \frac{1 + y + y^2 - y^3}{(1 - y)^3} \tag{6}$$

The contact value of the pair-correlation function is

$$g_{HS}(\sigma) = \frac{2 - y}{2(1 - y)^3} \tag{7}$$

The contact value of the diatomic fluid is given by[50]

$$g_{HD}(\sigma) = \frac{1 + 2y}{2(1 - y)^2} \tag{8}$$

Figure 3 shows the equation-of-state data obtained from MC simulations[38−40] for linear, tangent hard-sphere chains with 16, 51, and 201 spheres. The solid line represents the predictions of the TPT-D1 equation of state for an infinitely long polymer chain (i.e., $N \rightarrow \infty$). The equation of state of a monomer hard-sphere fluid, calculated with the Carnahan−Starling equation of state, eq 6, is shown with a dashed line. The pressure of the fluids composed of chain molecules is lower than that of the monomer hard-sphere fluid at the same packing fraction. This lowering of the pressure is due to the bonds that connect the spheres in the chain fluid. These bonds can be thought of as an attractive force between the spheres, which lowers the pressure.

For moderate-to-high packing fractions (greater than 0.1), the equation of state rapidly approaches a "universal" limiting form, which is independent of the length of the chain. The equations of state are almost the same for the 16, 51, and 201-sphere chain systems. The TPT-D1 equation of state for infinitely long chains (solid line) compares very well with the MC data.

For the concentrated hard-sphere chain system, the major contributions to the thermodynamic properties are the excluded-volume interactions and the bonding constraint. For moderately concentrated systems, the correlations induced by the intramolecular bonds between different spheres of the same molecule are significantly screened if the molecules of the system can easily interpenetrate. Physically, this means that only bonds in close proximity to a sphere influence its behavior. Therefore, the manner in which the molecules are bonded, that is, the architecture of the molecules, is no longer important. This accounts for the success of polymer theories that take into account bonding on only a local level.

As in the case of linear polymer solutions, we expect to observe the dilute and concentrated regimes for dendritic polymers in good solvents. However, only dendritic polymers with very large separator lengths will exhibit a semidilute regime. This is due to the fact that the semidilute regime appears only for solutions containing large extended molecules, such as linear polymers. In this regime, the molecules interact significantly with each other, even though the volume fraction of space that they occupy is extremely low. Nearly all of the currently synthesized dendrimers do not have significantly long separator lengths and, as a consequence, are rather compact objects (as compared to linear chains). Therefore, we do not expect to experimentally observe a semidilute regime for these molecules.

The previous argument was based on the assumption that the molecules in the system could easily interpenetrate. For low-generation-number dendrimers, this assumption is satisfied, and, as will be shown in the next section, the equation of state is similar to that of the linear chain. However, high-generation-number dendrimers are fairly dense, owing to their hyperbranched architecture, and, as a result, they cannot easily interpenetrate. In this case, the equation of state differs from that of the linear chain.

4. Results and Discussion

In Table 2, we report the mean-square radius of gyration $\langle R_g^2 \rangle$ and the second-virial coefficient B_2 for dendrimers of generations 0−5 and for linear chains with the same number of spheres (N) as the dendrimers. As a consequence of the hyperbranched architecture of the dendritic polymers, the $\langle R_g^2 \rangle$ and the B_2 for the dendrimers are lower than those for the corresponding linear polymers. Therefore, the linear chains are larger, more extended objects, where the dendrimers are more compact, dense objects. In addition, since B_2 for the linear polymers is larger than that for the dendritic polymers, for dilute systems the osmotic pressure of dilute linear polymer solutions is expected to be higher than that of the corresponding dendritic polymer solutions.

Figure 4 shows the mean-density profile of a generation-2 dendrimer molecule ($N = 43$) at four packing fractions ($y = 0$, 0.1, 0.2, and 0.3).

The abscissa represents the distance from the dendrimer center of mass, and the ordinate is the average local sphere density. For the isolated dendrimer ($y = 0$), there is a small shoulder at about 1.5−2 σ, a consequence of the hyperbranched architecture of the dendritic polymer. As the concentration of dendrimers in solution increases, the dendrimers become more

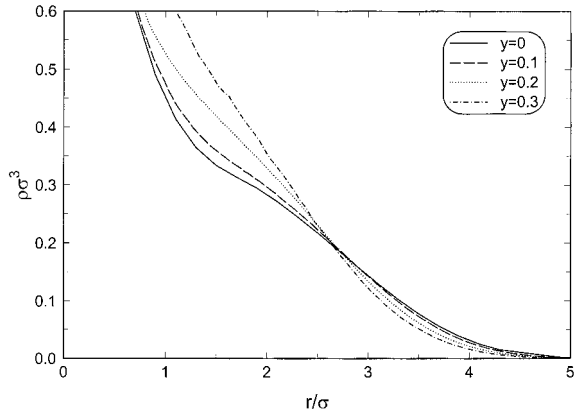

Figure 4. Density profile of generation-2 dendrimers at (i) $y = 0$ (solid line), (ii) $y = 0.1$ (dashed line), (iii) $y = 0.2$ (dotted line), and (iv) $y = 0.3$ (dash−dotted line).

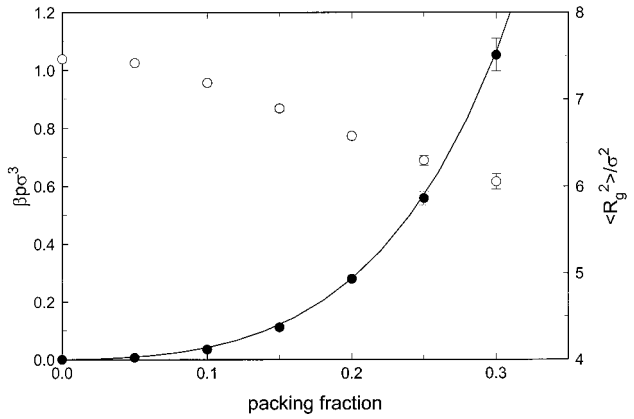

Figure 5. Equation of state (solid circles) and mean-square radius of gyration (open circles) for a generation-2 dendrimer. The solid line represents the prediction of the TPT-D1 model for an infinitely long tangent hard-sphere chain.

compact owing to collisions with other dendrimers. This compression of the dendrimer molecule is accompanied by the loss of the shoulder in the density profile. This compaction of the dendrimer can also be seen (Figure 5) in the radius of gyration, which decreases slightly with increasing dendrimer concentration.

In Figure 5, we plot our MC results for the pressure of the generation-2 dendrimer systems. As a comparison, we also plot (solid line) the predictions of the TPT-D1 equation of state for infinitely long linear chains ($N \rightarrow \infty$). The simulation data for the generation-2 dendrimers are well described by this curve. Therefore, at moderate-to-high concentrations, low-generation dendrimer solutions do not behave very differently from linear polymers.

In the concentrated regime, the polymers are highly interpenetrated and the monomers in the chain exist in a fairly crowded environment. In this situation, the major forces felt by a monomer are the excluded volume interactions exerted by other nearby monomers and the forces due to its chemical bonds. Note that the dendrimer and the linear chain of the same molecular weight (N) possess the same number of molecular bonds ($N - 1$). In this regime, the overall architecture of the polymer does not play a significant role in determining the thermodynamics of the system.

Figure 6 gives the density distribution about the center of mass for generation-5 dendrimers ($N = 379$) at packing fractions ranging from 0 to 0.3. The isolated molecule ($y = 0$) has a hollow region around $r/\sigma \approx 2$ and

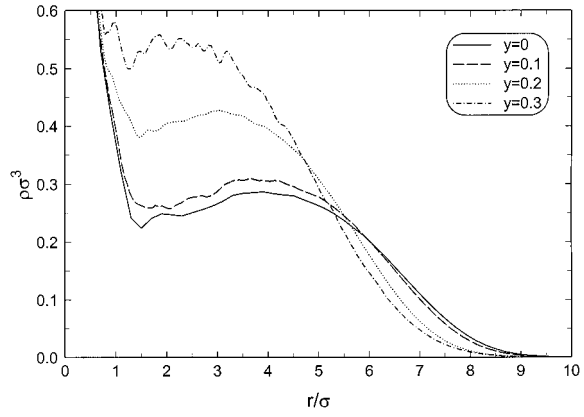

Figure 6. Density profile of generation-5 dendrimers at (i) $y = 0$ (solid line), (ii) $y = 0.1$ (dashed line), (iii) $y = 0.2$ (dotted line), and (iv) $y = 0.3$ (dash−dotted line).

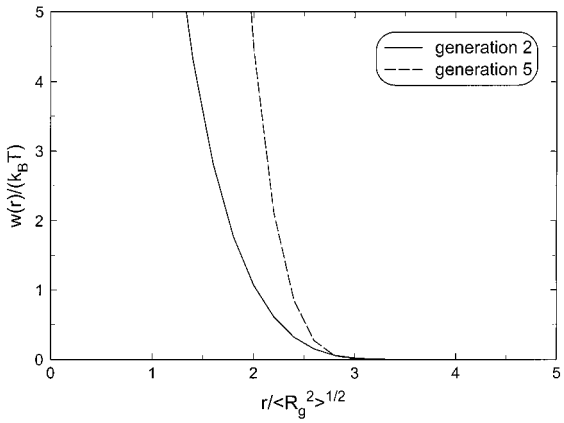

Figure 7. Potential of mean force between dendritic polymers at infinite dilution: (i) generation 2 (solid line) and (ii) generation 5 (dashed line).

a denser shell at $r/\sigma \approx 4$. This general structure is characteristic of high-generation dendrimers and is a consequence of the hyperbranched architecture. The presence of the dense shell hinders the ability of the dendrimers to interpenetrate each other.

The density profile does not change very much for dendrimer volume fractions of up to $y = 0.1$. However, at $y = 0.2$, the dense shell becomes compressed, and at $y = 0.3$ the hollow region is greatly reduced. This should be compared to the change with y of the density distribution for the generation-2 dendrimer (Figure 5). The generation-2 dendrimers were not as significantly compressed because they are more readily interpenetrable. On the other hand, the presence of the dense shell (Figure 6) in higher-generation dendrimers forces the molecules to compress one another without possibility of interpenetration. Correspondingly, the mean-square radius of gyration (Figure 8, open circles) shows a steep decrease at $y \approx 0.15$.

In Figure 7, we plot the simulation results for the potential of mean force $w(r)$ between generation-2 (solid line) and generation-5 (dashed line) dendrimers at infinite dilution. The potential of mean force is defined as the free energy required to bring the center of masses of two molecules from infinite separation to a distance r apart. The potential of mean force for the generation-2 dendrimers increases less steeply than that for the generation-5 dendrimers, again demonstrating that the generation-2 dendrimers are more interpenetrable.

Figure 8 compares the pressure of generation-5 dendrimers (solid circles) from MC simulations to the

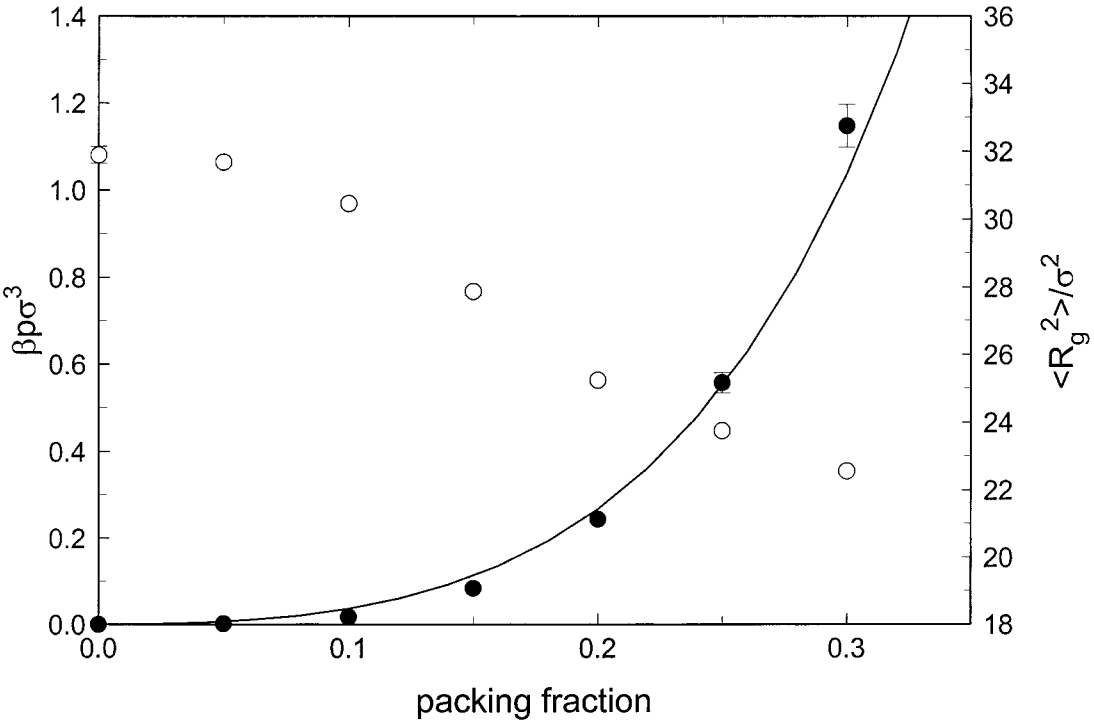

Figure 8. Equation of state (solid circles) and mean-square radius of gyration (open circles) for a generation-5 dendrimer. The solid line represents the prediction of the TPT-D1 model for an infinitely long tangent hard-sphere chain.

pressure of infinitely long linear chains calculated using the TPT-D1 equation of state (solid line). At low packing fraction, the pressure of dendrimers is lower than that of linear polymers because the structure of isolated molecules is more compact for dendrimers than for linear chains. This is consistent with the second-virial coefficient being lower for dendrimers (Table 2). At higher packing fractions (above 0.2), the behavior changes. For generation-5 dendrimers, the pressure is higher than that of linear molecules because linear chains are more compressible and are able to interpenetrate each other more easily, thus lowering the pressure of the system.

In this work, we have only investigated dendrimers with a three-functional core, bifunctional branching points, and a separator length of two (two spheres between branching points). Changing these parameters would lead to different results, although we anticipate that they would be qualitatively similiar. For example, by increasing (decreasing) the functionality of the core, increasing (decreasing) the number of branches, or decreasing (increasing) the separator length, the differences between thermodyamic properties of moderately concentrated linear and dendritic polymer solutions would be found at lower (higher) generations. This is because the "degree of crowding" within each dendrimer molecule would increase (decrease), making it more (less) difficult for the dendrimer molecules to interpenetrate.

However, we still expect that below a certain "critical" generation number (dependent on the architectural details of the dendrimer), this difference would disappear. In addition, for very dilute polymer concentrations, the osmotic pressure of the dendritic polymer solution will be lower than that of the corresponding linear polymer solution, for all generation numbers.

5. Conclusions

We have performed Monte Carlo simulations for athermal dendritic polymers from generation 0 to generation 5. The computed properties included the second-virial coefficient, the mean-square radius of gyration, the density profile, and the equation of state.

Because of the compact structure, the second-virial coefficients of the dendritic polymers are much lower than those of linear chains of the same molecular weight. Consequently, the pressures of dilute dendritic polymers are much lower than those for linear polymers. The effect becomes more pronounced with increasing generation number.

From moderate to high concentrations, the equations of state of the lower-generation dendrimers behave similarly to that of linear chains. At these conditions, dendrimers of higher generation number tend to deviate from the results of linear chains. This is due to the inability of the dendrimers to easily interpenetrate each other, a result of their hyperbranched architecture. As a result, at high concentrations the pressure of the dendrimer becomes higher than that of the corresponding linear chain. This effect increases with increasing generation number and decreasing separator length.

Acknowledgment. The author thanks Dr. C. Mio, Dr. A. Laesecke, and Prof. J. R. Elliott for helpful comments and suggestions.

References and Notes

(1) Newkome, G. R.; Moorefield, C. N.; Vögtle, F. *Dendritic Molecules: Concepts, Synthesis, Perspectives*; VCH: Weinheim, 1996.
(2) Tomalia, D. A.; Durst, H. D. *Top. Curr. Chem.* **1993**, *165*, 193−313.
(3) Frechet, J. M. J.; Hawker, C. J. In *Comprehensive Polymer Science*, 2nd suppl., Aggarwal, S., Russo, S., Eds.; Pergamon Press: Oxford, 1996; pp 234−298.

(4) Nunez, C. M.; Andrady, A. L.; Guo, R. K.; Baskir, J. N.; Morgan, D. *J. Polm. Sci., Part A, Polm. Chem.* **1998**, *36*, 2111−2117.
(5) Knapen, J. W. J.; van der Made, A. W.; de Wilde, J. C.; van Leeuwen, P. W. N. M.; Wijkens, P.; Grove, D. M.; van Koten, G. *Nature* **1994**, *372*, 659−663.
(6) Jansen, J. F. G. A.; de Brabander-van den Berg, E. M. M.; Meijer, E. W. *Science* **1994**, *266*, 1226−1229.
(7) Jansen, J. F. G. A.; Meijer, E. W.; de Brabander-van den Berg, E. M. M. *J. Am. Chem. Soc.* **1995**, *117*, 4417−4418.
(8) Zimmerman, S. C. *Curr. Opin. Colloid Interface Sci.* **1997**, *2*, 89−99.
(9) Miller, L. L.; Kunugi, Y.; Canavesi, A.; Rigaut, S.; Moorefield, C. N.; Newkome, G. R. *Chem. Mater.* **1998**, *10*, 1751−1754.
(10) Hawker, C. J.; Wooley, K. L.; Frechet, J. M. J. *J. Am. Chem. Soc.* **1993**, *115*, 4375−4376.
(11) Moreno-Bondi, M. C.; Orellana, G.; Turro, N. J.; Tomalia, D. A. *Macromolecules* **1990**, *23*, 910−912.
(12) Prosa, T. J.; Bauer, B. J.; Amis, E. J.; Tomalia, D. A.; Scherrenberg, R. *J. Polym. Sci.* **1997**, *35*, 2913−2924.
(13) Scherrenberg, R.; Coussens, B.; vanVliet, P.; Edouard, G.; Brackman, J.; deBrabander, E. *Macromolecules* **1998**, *31*, 456−461.
(14) Hawker, C. J.; Farrington, P. J.; Mackay, M. E.; Wooley, K. L.; Frechet, J. M. J. *J. Am. Chem. Soc.* **1995**, *117*, 4409−4410.
(15) Uppuluri, S.; Keinath, S. E.; Tomalia, D. A.; Dvornic, P. R. *Macromolecules* **1998**, *31*, 4498−4510.
(16) Wooley, K. L.; Hawker, C. J.; Pochan, J. M.; Frechet, J. M. J. *Macromolecules* **1993**, *26*, 1514−1519.
(17) Mourey, T. H.; Turner, S. R.; Rubinstein, M.; Frechet, J. M. J.; Hawker, C. J.; Wooley, K. L. *Macromolecules* **1992**, *25*, 2401−2406.
(18) Ramzi, A.; Scherrenberg, R.; Brackman, J.; Joosten, J.; Mortensen, K. *Macromolecules* **1998**, *31*, 1621−1626.
(19) Mio, C.; Kiritsov, S.; Thio, Y.; Brafman, R.; Prausnitz, J. M.; Hawker, C.; Malmstrom, E. E. *J. Chem. Eng. Data* **1998**, *43*, 541−550.
(20) de Gennes, P. G.; Hervet, H. *J. Phys.* **1983**, *44*, L351−L360.
(21) Boris, D.; Rubinstein, M. *Macromolecules* **1996**, *29*, 7251−7260.
(22) Biswas, P.; Cherayil, B. J. *J. Chem. Phys.* **1994**, *100*, 3201−3209.
(23) Naylor, A. M.; Goddard, W. A.; Kiefer, G. E.; Tomalia, D. *J. Am. Chem. Soc.* **1989**, *111*, 2339−2341.
(24) Mansfield, M. L.; Klushin, L. I. *Macromolecules* **1993**, *26*, 4262−4268.
(25) Murat, M.; Grest, G. S. *Macromolecules* **1996**, *29*, 1278−1285.
(26) Chen, Z. Y.; Cui, S.-M. *Macromolecules* **1996**, *29*, 7943−7952.
(27) Lue, L.; Prausnitz, J. M. *Macromolecules* **1997**, *30*, 6650−6657.
(28) Nemirovski, A. M.; Bawendi, M. G.; Freed, K. F. *J. Chem. Phys.* **1987**, *87*, 7272−7284.
(29) Dudowicz, J.; Freed, K. F.; Madden, W. G. *Macromolecules* **1990**, *23*, 4083−4819.
(30) Yethiraj, A.; Hall, C. K. *J. Chem. Phys.* **1991**, *94*, 3943−3948.
(31) Gujrati, P. D. *Phys. Rev. Lett.* **1984**, *74*, 1367−1370.
(32) Hu, Y.; Liu, H.; Prausnitz, J. M. *J. Chem. Phys.* **1996**, *104*, 396−404.
(33) Escobedo, F. A.; dePablo, J. J. *J. Chem. Phys.* **1996**, *104*, 4788−4801.
(34) Dautenhahn, J.; Hall, C. K. *Macromolecules* **1994**, *27*, 5399−5412.
(35) Escobedo, F. A.; dePablo, J. J. *J. Chem. Phys.* **1995**, *102*, 2636−2652.
(36) Frenkel, D.; Smit, B. *Understanding Molecular Simulation: From Algorithm to Applications*; Academic Press: San Diego, CA, 1996.
(37) Eppenga, R.; Frenkel, D. *Mol. Phys.* **1984**, *52*, 1303−1334.
(38) Dickman, R.; Hall, C. K. *J. Chem. Phys* **1988**, *89*, 3168−3174.
(39) Gao, J.; Wiener, J. H. *J. Chem. Phys.* **1989**, *91*, 3168−3173.
(40) Denlinger, M. A.; Hall, C. K. *Mol. Phys.* **1990**, *71*, 541−559.
(41) de Gennes, P. G. *Scaling Concepts in Polymer Physics*; Cornell University Press: Ithaca, NY, 1979.
(42) Grosberg, A. Y.; Khokhlov, A. R. In *Statistical Physics of Macromolecules, AIP Series in Polymers and Complex Materials*; Larson, R., Pincus, P. A., Eds.; AIP Press: New York, 1994.
(43) Wertheim, M. S. *J. Chem. Phys.* **1987**, *87*, 7323−7331.
(44) Honnell, K. G.; Hall, C. K. *J. Chem. Phys.* **1989**, *90*, 1841−1855.
(45) Chiew, Y. C. *Mol. Phys.* **1990**, *70*, 129−143.
(46) Ghonasgi, D.; Chapman, W. G. *J. Chem. Phys.* **1994**, *100*, 6633−6639.
(47) Chang, J.; Sandler, S. I. *Chem. Eng. Sci.* **1994**, *49*, 2777−2791.
(48) Stell, G.; Lin, C.-T.; Kalyuzhnyi, Y. V. *J. Chem. Phys.* **1999**, *110*, 5444−5457.
(49) Carnahan, N. F.; Starling, K. E. *J. Chem. Phys.* **1969**, *51*, 635−636.
(50) Chiew, Y. C. *Mol. Phys.* **1991**, *73*, 359−373.

MA991340B